

Article

Dynamic Bath Mixing during an Ingot Casting Process

Xiaobin Zhou ^{1,2}, Liangcai Zhong ³, Peiyuan Ni ^{3,4} and Nanyang Deng ^{1,*}

¹ School of Metallurgical Engineering, Anhui University of Technology, Ma'anshan 243032, China; zxbahut@163.com

² Key Laboratory of Metallurgical Emission Reduction & Resources Recycling, Ministry of Education, Anhui University of Technology, Ma'anshan 243032, China

³ School of Metallurgy, Northeastern University, Shenyang 110819, China; zhonglc@126.com (L.Z.); peiyuann@kth.se (P.N.)

⁴ Division of Materials and Manufacturing Science, Graduate School of Engineering, Osaka University, 2-Yamadaoka, Osaka 565-0871, Japan

* Correspondence: xiaobinzahut@163.com; Tel.: +86-189-5553-6370

Received: 30 January 2019; Accepted: 13 February 2019; Published: 17 February 2019



Abstract: This paper presents the results of a bath stirring investigation using a physical model for an uphill ingot casting process. A new method of mixing time measurement that overcomes the drawback of the conventional measurement method was developed. The method was used to investigate bath stirring for a dynamic-volume bulk bath in which the liquid volume increases over time during the teeming process. The results show that the new method can be successfully applied to reveal the relationship between gas blowing schemes, gas blowing flowrates, and bath depths. It is demonstrated that blowing bubbles causes the flow of the bath to increase when the bath depth is increased. By applying the new data analysis method, three different bottom blowing schemes were explored to study the mixing behaviors under different operating conditions. The results suggest that the concentric circular annulus is more favorable than both the eccentric blowing scheme and symmetrical scheme to achieve efficient mixing.

Keywords: steel ingot casting; physical model; gas blowing mixing; dynamic process

1. Introduction

Ingot casting remains an important process for the production of certain steel grades for special applications, and it is a necessary addition to the continuous casting process in steel production. The uphill teeming process, which is suitable for the production of high-quality steels, is a widely applied ingot casting method whereby molten steel flows through a runner to an inlet nozzle located at the bottom of the mold.

In order to realize efficient steel production, gas injection is widely used in the steelmaking and casting process for various aims, such as homogenizing the metal bath for both temperature and composition, removing nonmetallic inclusions, removing harmful hydrogen, and so on. The bubble flow formed in metallurgical vessels, such as ladles, tundishes, and continuous casting molds, has been investigated and proved to be useful not only for making the composition and temperature uniform but also for removing inclusions [1–3]. It is well known that nonmetallic inclusions are a significant problem because inclusions in the ingot can decrease the ductility, fracture toughness, and resistance to hydrogen-induced cracks. The typical mechanism for the removal of inclusions during a gas treatment is by attaching to the bubble surface and following the bubble tail, the flow transport, and the buoyancy effect. In addition, a high flow velocity at the steel/slag interface can

lead to slag entrainment, which will form new inclusions. Therefore, inclusions must be carefully removed during the teeming process. Many efforts have been devoted to optimizing the flow field of the bath to decrease the likelihood of flow shear-induced slag entrapment by developing different types of nozzles for the process [4–7]. The casting mold is the last chance to remove these inclusions, and the probability of successful inclusion removal may be enhanced by introducing a bubble flow to the ingot mold. Furthermore, gas injection also helps to homogenize the composition and temperature of the bath for the ingot mold. To understand the effects of the introduced bubbling flow on the flow behaviors of the bath, mixing time is a typical characteristic used to reflect the bath stirring process under different operation conditions.

Mixing time experiments have been applied in bath stirring investigations not only in metallurgy vessels [8–10] but also in other chemical industries [11,12] that involve agitated baths. A number of mixing time measurements in stirred vessels under either single or multiphase flow simulations have been summarized in the literature [13] to review experimental techniques. In the past decades, many techniques, such as colorimetry [14], the thermography principle [15], conductometry [16], and pH (pondus hydrogenii) [17], have been developed to improve the reliability of measuring mixing time. Moreover, with the development of computer technology, mathematical models are being applied to investigate the mixing phenomena for the stirred bath [11,14,18–20]. Mostly, the mixing times mentioned in most of the literature are the times required to achieve the desired degree of homogenization. One exception [18] to this characterization is the definition of mixing time as the time needed to achieve 99% homogenized volume of the tracer over the entire bath volume; defining it in this way overcomes a drawback of the common measurement method: i.e., the location of the “dead zone” is difficult to estimate and measure.

A remarkable characteristic of the stirred vessels mentioned in most of the literature is that the volume of the liquid in the bath is a constant value. In the current study, the ingot casting teeming process is a dynamic process in which the bath liquid increases during the teeming process until the procedure is finished. Therefore, the traditional method of mixing time measurement and data analysis to characterize the mixing of the bath is not appropriate for a dynamic process. However, mixing time measurement has been rarely reported for a dynamic chemical process in which the volume of the liquid varies and the bath stirring process is important. Consequently, the main purpose of this research is to develop a new data analysis method to investigate bath stirring when agitated by bottom blowing using a physical model that was built on the basis of a 30 t ingot mold. In addition, the blowing location was considered to prevent bubbles from being captured by lining refractory. The effects of different schemes of bottom blowing on the bath stirring process for a transient ingot teeming process were investigated.

2. Experimental Apparatus and Procedure

To accommodate a 30 t industrial ingot mold (China Baowu Steel Group Corporation Limited, Shanghai, China), a 1/3 scaled down physical model, as shown in Figure 1 and described in previous research [21], was used to investigate the stirring of the bath when bottom blowing was introduced. In the current study, measurement of the mixing time was performed by applying the experimental apparatus shown in Figure 2. A solution of 0.2 g/mL NaCl was employed as the tracer to measure the mixing behavior in the bath, while red ink was applied as the tracer to show the movement of the inlet flow from the nozzle. Three conductivity probes were set at different locations in the bath. The signals acquired by the probes were recorded by a computer through the conductivity acquisition system.

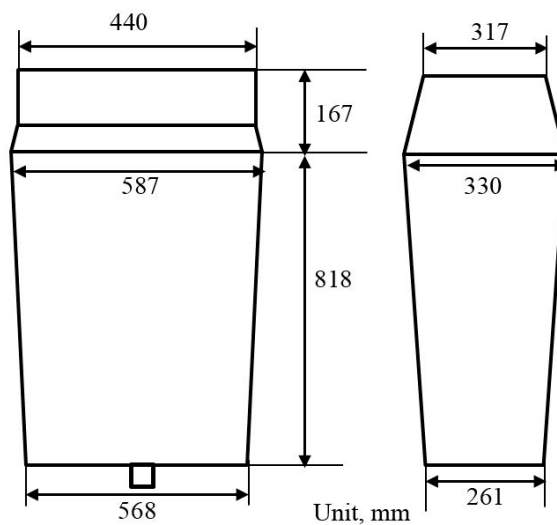


Figure 1. Dimensions of the physical model (unit, mm).

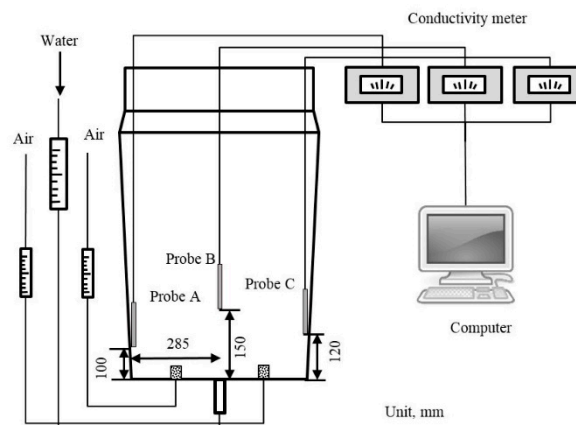


Figure 2. Schematic of the mixing time measurement system.

Traditionally, a mixing time investigation for a bath using a water model includes measuring the variation in tracer concentration at several different measurement positions in the bath. The volume of the liquid in the bath is constant. On the contrary, the liquid volume in the bath of the ingot mold increases with teeming time during an ingot casting process. In a previous study [21], bath mixing times were studied at different bath depths, which was stable when the tracer was added into the bath. Namely, the tracer was added into the bath when the bath depth increased to the target depth, and the teeming was stopped. The mixing behavior in that type of bath is different from that in a dynamic process. In the current study, mixing behaviors were investigated for different bath depths, where each one is considered the initial bath depth while the teeming process is occurring. A new method to evaluate the mixing in such a dynamic process was applied, as described below.

As shown in Figure 3, the tracer was added into the bath when the bath depth reached the specified initial depth (H_1). At the same time, the measurement process began, and the teeming process did not end until the bath depth reached a preset depth (H_2) in order to allow certain mixing of the tracer with the current flow pattern. The teeming time from initial depth H_1 to final depth H_2 was recorded, and then the measurement continued until the bath was homogeneous. Also, the data analysis was very different from that of the previous traditional method. More detail is given in the Discussion section. On the basis of the developed measurement method, the effects of different schemes on the mixing time of the bath were investigated to assess bottom blowing.

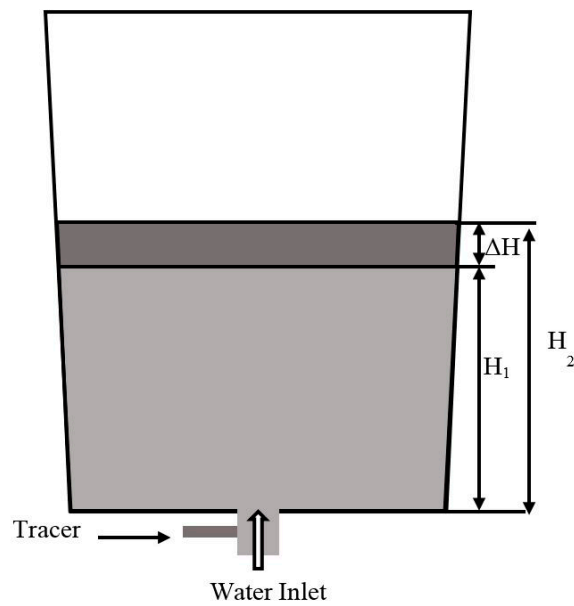


Figure 3. Schematic of the investigating method.

Figure 4 shows the flow patterns for the same time point (5 s) after the tracer was injected in different bath depths. As shown in the figure, the flow patterns differ in different bath depths. Apparently, a flow pattern in a bath depth is not representative of the flow field for the whole teeming process during the ingot casting teeming process. In light of this, several different bath depths, which are expected to reflect the bath stirring for different parameters, were chosen to study the mixing behaviors of the bath for different teeming stages, as shown in Table 1. The tracer quantities, as well as the depth increase ΔH , were changed according to different bath depths in consideration of measurement accuracy.

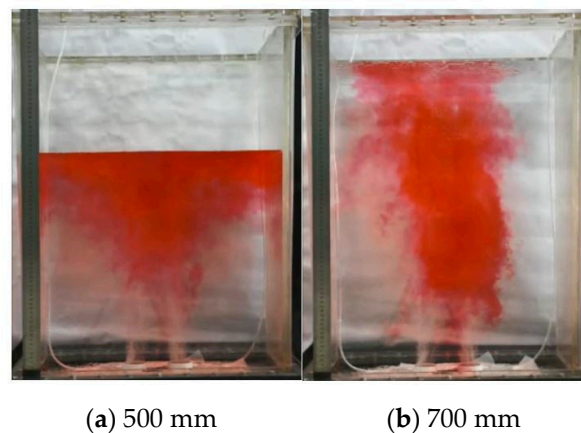
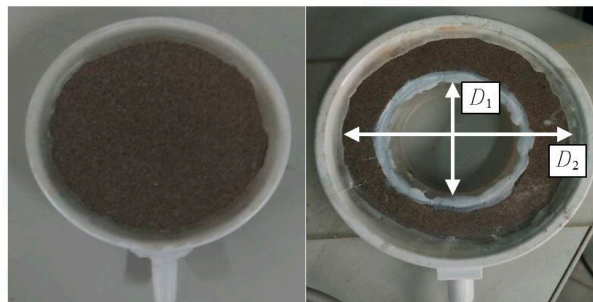


Figure 4. Tracer patterns in different teeming depths.

Table 1. Parameters used in the experiments.

Teeming flowrate, m ³ /h	0.8		
Gas flowrate, Nm ³ /h	0.025, 0.045, 0.065		
Initial bath depth, mm	300	500	700
Tracer, mL	100	170	240
ΔH , mm	50	80	120

To investigate the effects of different bottom blowing schemes on the flow patterns, as well as mixing behaviors of the bath, three different schemes were chosen in the current study, as shown in Figures 5 and 6. Circular porous bricks with a diameter of 50 mm were applied in the experiment to form an eccentric blowing scheme (Figure 6a) and a symmetrical blowing scheme (Figure 6b). Also, a concentric circular annulus (Figure 6c) was applied as another blowing scheme. Considering the practical conditions, porous bricks applied in the physical model were designed to be arranged closely with the teeming nozzle to prevent bubbles from being captured by the solidification shell in reality.



(a) $D = 50$ mm (b) $D_1 = 60$ mm, $D_2 = 85$ mm

Figure 5. The porous plug used in the physical model.

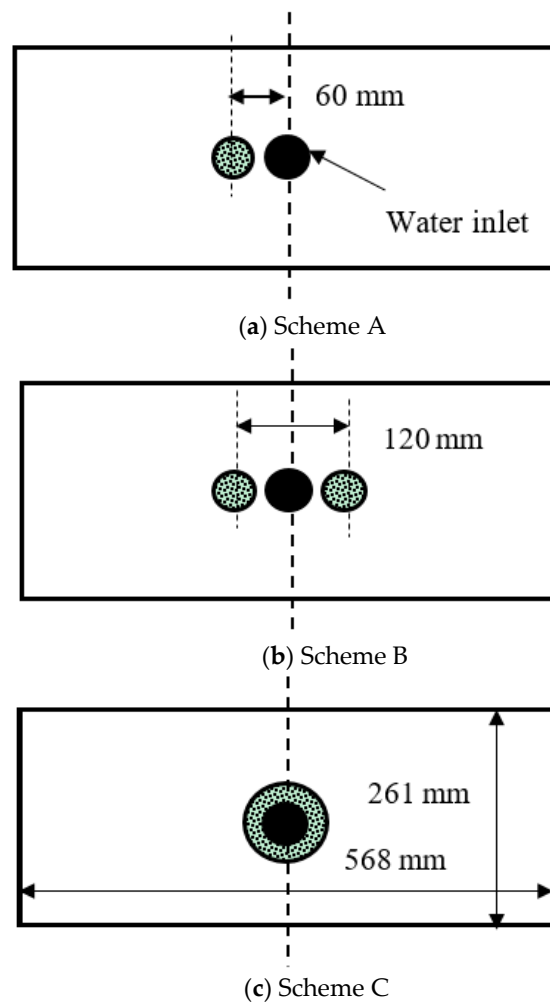


Figure 6. Top-view schemes of the bottom-blowing plug.

3. Results and Discussions

In the current study, a new experimental method was applied, and the acquired data were analyzed to reveal the mixing behaviors of the bath under different operational conditions. On the basis of the new method, three different bottom blowing schemes were used to investigate the effects of blowing schemes and blowing flowrates on the mixing time of the bath.

3.1. Mixing Phenomena Analyses Method

Traditionally, mixing time is considered to be the time required for the injected tracer to become homogeneous in a stirred bath, and the volume of the bulk liquid is fixed. However, the volume of the bulk liquid in the teeming process of the ingot is not constant; namely, the volume of the liquid increases throughout the whole teeming process. As a result, the flow patterns in a dynamic bath will differ from those in a fixed bath when the injected flow from the nozzle is stopped, as shown in Figure 7. The figure shows the tracer's movement 2 s and 5 s after the tracer was injected into the bath at a bath depth of 500 mm for fixed and dynamic depths using Scheme B for bottom blowing. There are apparent differences in the tracer's movement in the bath between the fixed and dynamic bath. This demonstrates that mixing time measurement for the ingot casting process cannot be performed in the same way as that of vessels like a ladle, since a strictly homogeneous bath does not exist during the process because the liquid is injected continuously from the bottom of the model. So, a new data analysis method was necessary to investigate bath stirring in the physical model for the ingot teeming process.

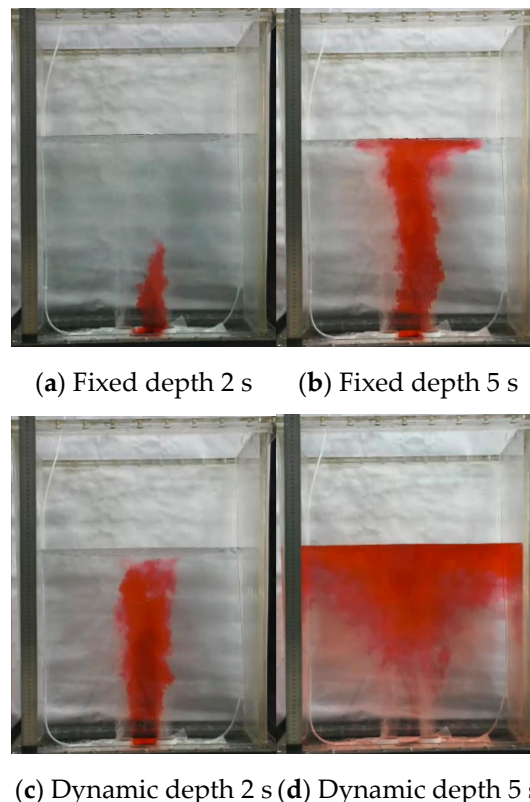


Figure 7. Tracer patterns in different measurement methods.

Figure 8 shows typical tracer concentration measurements for the physical model during the dynamic teeming process. The concentration of the tracer at the measurement location is represented by the local conductivity of the bath. As described in the experimental section, the valid measurement of the curves starts when the tracer is injected into the bath and continues until the time at which

the teeming stops. Further measurement after the teeming ends is used to achieve homogeneous conditions for reference in the analysis step.

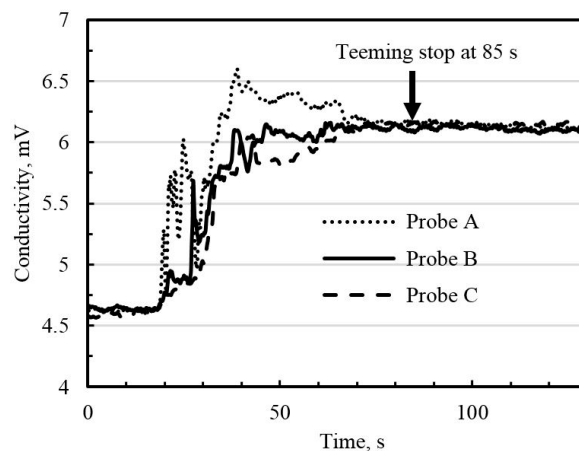


Figure 8. Typical tracer homogeneous curves in different probes.

The curve measured by probe C in Figure 8 is extracted and shown in Figure 9. The measurement was performed when the bath depth was 700 mm with a gas flowrate of $0.065 \text{ Nm}^3/\text{h}$ using Scheme B. The tracer was injected into the bath when the bath depth was 700 mm. Once the bath depth increased to 820 mm, the teeming stopped, and the time of 85 s was recorded. Measurements were taken continuously until the bath was homogeneous with the help of bottom blowing.

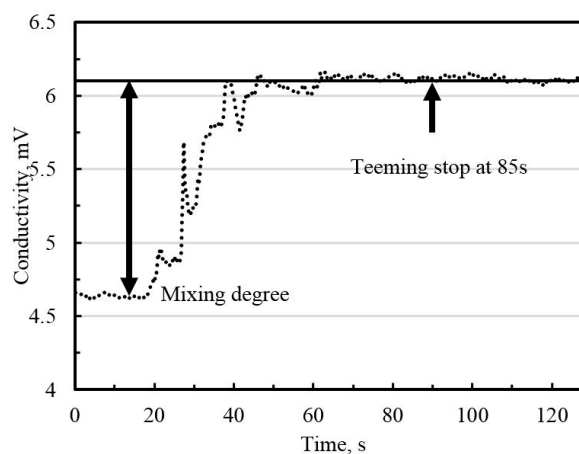


Figure 9. Typical tracer homogeneous curves in different probes.

Since the bath is not completely homogeneous when the teeming is stopped, the traditional concept of “mixing time” is not appropriate for characterizing the stirring condition of the bath. So, a “mixing degree”, which describes the concentration difference between the concentration measured at the probe and the theoretically homogeneous concentration at the measurement moment, was developed to reflect the transient stirring condition of the bath. Note that the theoretical homogeneous concentration, which changes with increasing bath volume, has a one-to-one correspondence to the measured concentration at any moment. To simplify the “mixing degree” calculation, a final homogeneous concentration that corresponds to the final bath depth (H_2) was applied instead of the theoretical homogeneous concentration in transient measurements. An average value of the “mixing degree” at all measurement instances (from the start of the measurements to the time that teeming stops) was adopted to describe the stirring condition of the bath. Therefore, a lower

mixing degree corresponds to a more efficient bath stirring condition. The mixing degree is calculated as the equation shown below:

$$I_m = \frac{1}{n} \sum_{i=1}^n \frac{|C_i - C_0|}{C_0} \quad (1)$$

where I_m is the mixing degree, which is a dimensionless number; n is the number of measurements in the data; C_i is a transient concentration at any measurement moment; C_0 is the homogeneous concentration for the final bath depth (H_2).

3.2. Effects of Gas Flowrate on the Flow Behavior in the Bath

Three different flowrates of bottom gas blowing, with values of 0.025, 0.045, and 0.065 Nm³/h, were explored for the bottom blowing schemes in the physical simulation. Figure 10 shows the tracer patterns 5 s after tracer injection with different bottom blowing flowrates at a bath depth of 500 mm using Scheme B. As shown in the figure, the tracer flows to the upper part of the bath after it is injected from the inlet nozzle. The tracer moves more quickly when the bottom gas blowing flowrate increases. This indicates that the rising bubbles formed by bottom blowing are favorable for bath stirring. To further investigate the effect of bottom blowing on bath stirring, the NaCl solution was injected into the bath from the top/surface of the bath to measure the concentration change in the tracer at different locations. The data measured by Probe B were extracted to clearly show the effects of the gas flowrate on the mixing intensity of the bath, as shown in Figure 11.

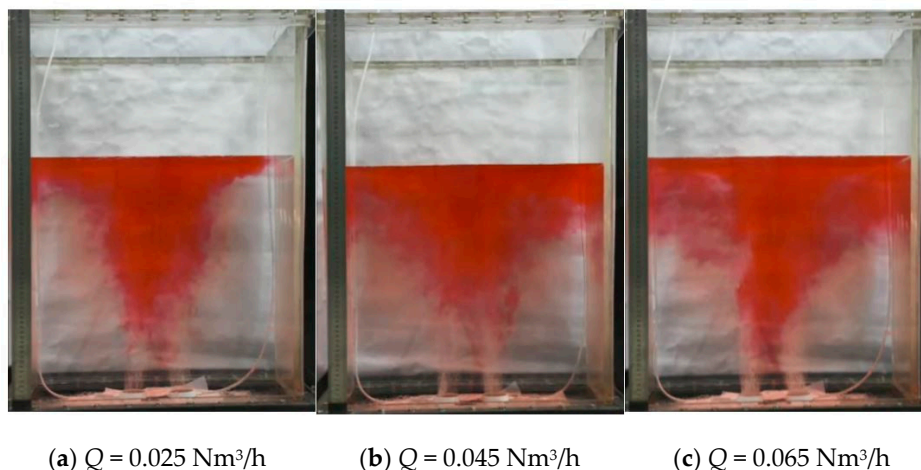


Figure 10. Tracer patterns as a function of bottom blowing flowrates at a bath depth of 500 mm.

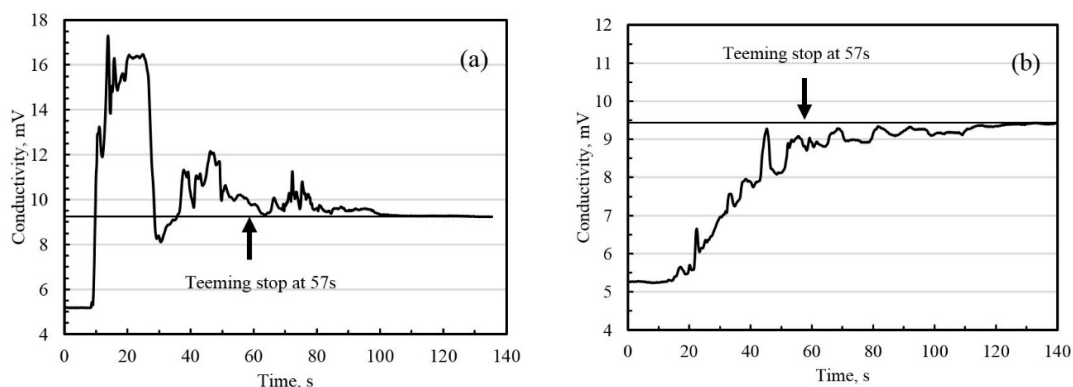


Figure 11. Cont.

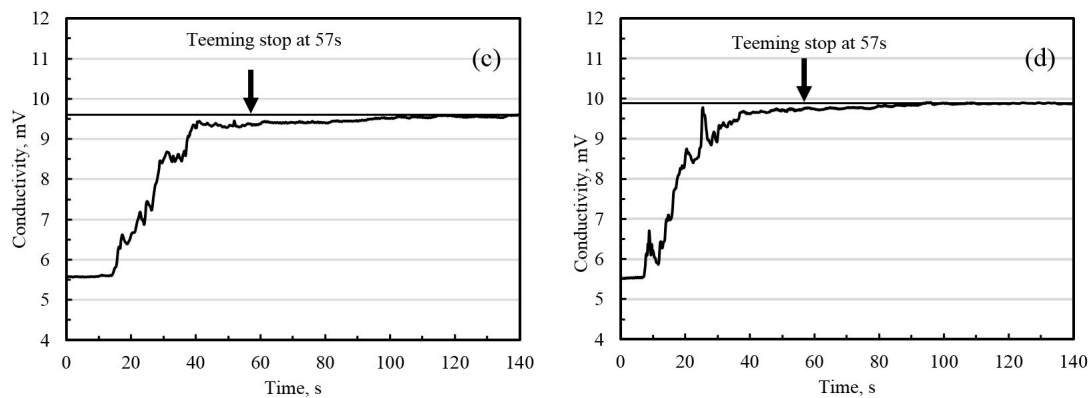


Figure 11. Measurement differences of the tracer at a bath depth of 500 mm; (a) $Q = 0$, (b) $Q = 0.025$, (c) $Q = 0.045$, (d) $Q = 0.065$.

For a bath depth of 500 mm, the teeming stopped at 57 s after the tracer was injected into the bath. As a result, the data measured after 57 s was not analyzed since subsequent flow pattern was not influenced by the teeming liquid flow since teeming had ended. Note that the homogeneous concentration measured after 57 s was used to draw a reference line for each data analysis. Figure 11a is the measurement of the tracer without bottom gas blowing for comparison with the cases of gas blowing. There are obvious differences in the relationship between the tracer concentration curve and the homogeneous line when the flow is not affected by bottom blowing. After introducing bottom blowing with a flowrate of $0.025 \text{ Nm}^3/\text{h}$, the shape of the measured curve changes visibly. To further investigate the effect of the gas flowrate on the curve's behavior, the gas flowrate was increased from 0 to $0.065 \text{ Nm}^3/\text{h}$. The results show that the tracer curve gets increasingly closer to the homogeneous line. A closer relationship between the tracer curve and the homogeneous line indicates good mixing in the bath. Accordingly, analyzing the differences between the tracer curve and the homogeneous line would reveal the tracer behavior, as well as the bath stirring process.

The data shown in Figure 11 were analyzed by Equation 1 and are shown in Figure 12, which reveals the relationship between the mixing degree and the bottom blowing flowrate in the using Scheme B. A general trend can be seen: the mixing degree decreases when the bottom blowing flowrate increases. The mixing degree is 3.1 when bottom blowing is not introduced to the bath. With the effects of bottom blowing, the mixing degree decreases to 2.53, 1.96, and 1.48 for bottom blowing flowrates of 0.025, 0.045 and $0.065 \text{ Nm}^3/\text{h}$, respectively. When increasing the bubbles, the bubble plume spreads better and transfers more kinetic energy to the bath when the bath depth increases. Furthermore, the decreasing trend for the mixing time corresponds to the proximity of the tracer curve to the homogeneous line.

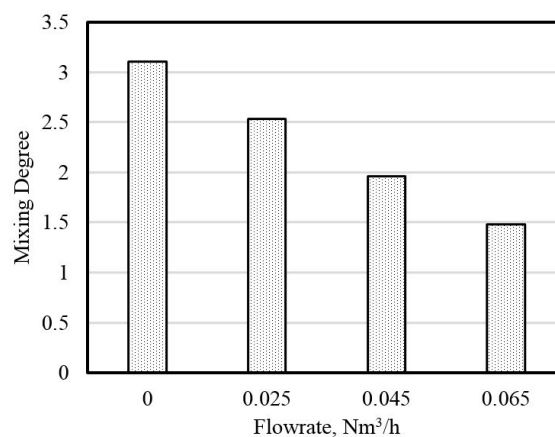


Figure 12. Mixing degree as a function of bottom blowing flowrate at a bath depth of 500 mm.

3.3. Mixing Time Investigation with Different Bottom Blowing Schemes

On the basis of the analytical approach mentioned above, three schemes of bottom blowing (shown in Figure 6) were investigated. The flow patterns were found not to be absolutely symmetrical, even if symmetrical blowing was applied. In addition, to reduce the measurement errors caused by manual operation and instrument measurement, the experiment was repeated three times to calculate the arithmetic average of the mixing degree, which is an average of the data acquired by three probes.

Before applying the bottom blowing schemes, three different bath depths were applied to investigate the mixing degree of the bath without gas blowing. As shown in Figure 13, the mixing degree for an initial depth of 300 mm is 1.9. The mixing degree increases to 2.9 and 3.7 when the initial bath depth increases to 500 and 700 mm, respectively. This provides the insight that it is more difficult to achieve homogeneity for a greater bath depth or a greater bath depth results in bath stirring with weaker intensity. By applying Scheme A for the bottom blowing, the mixing time decreases slightly when the gas flowrate increases from 0.025 to 0.065 Nm³/h at a bath depth of 300 mm. On the other hand, a mixing degree of 2.0 can be obtained when the gas flowrate is 0.025 Nm³/h when the bath depth is 500 mm. By increasing the bath depth to 700 mm, the mixing degree can be decreased to 1.8 with the same gas flowrate. Remarkably, no noticeable change in mixing degree can be found with further increases in the flowrate for all three bath depths. This indicates that the bath stirring process may be slightly affected when the blowing flowrate is higher than 0.025 Nm³/h for Scheme A. It suggests that the transfer efficiency of kinetic energy from the bubble plume to the bath decreases when a higher bottom blowing flowrate is introduced.

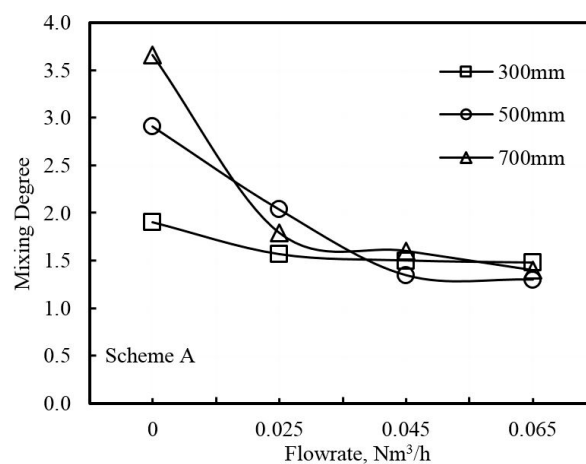


Figure 13. Mixing degree as a function of bottom blowing flowrate using Scheme A.

By performing a similar experimental process, the effect of Scheme B was investigated, and the results are shown in Figure 14. Generally, the mixing degree is a decreasing function of bottom blowing flowrate for all bath depths in the experiments. The highest mixing degree for each gas flowrate is measured at a bath depth of 700 mm, followed by the cases of 500 and 300 mm depths when the flowrate increases from 0 to 0.045 Nm³/h. When the flowrate increases to 0.065 Nm³/h, no noticeable difference in the mixing degree can be obtained for all three depths. Comparing the results shown in Figure 13, the mixing degrees are 10% and 61% higher than that of Scheme A when the flowrate is 0.025 Nm³/h at a bath depth of 500 and 700 mm, respectively. Also, when the flowrate increases to 0.045 Nm³/h, a 22% and 25% higher mixing degree can be found for bath depths of 500 and 700 mm, respectively. By comparing this with the results of Scheme A, it can be seen that the effect of the eccentric blowing scheme (Scheme A) is better than that of the symmetrical blowing scheme (Scheme B) on bath stirring according to the mixing degree results, because some of the energy resulting from the bubble plume is counteracted by the symmetrical flow. In addition, by considering the application in

practice, two bottom plugs were set near the inlet nozzle. The small distance between two plumes may cause more energy dissipation, which decreases the energy transfer from the plume to the bath.

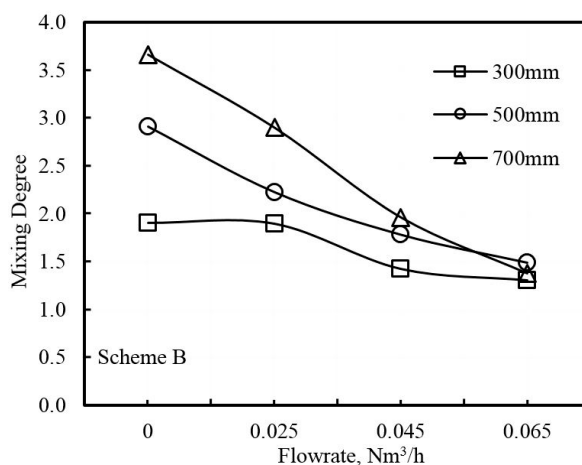


Figure 14. Mixing degree as a function of bottom blowing flowrate using Scheme B.

Remarkably, compared with the results of using Scheme B, the trend of mixing degree change with the bath depth is reversed by applying Scheme C: namely, the mixing degree decreases when the bath depth increases for each gas flowrate, as shown in Figure 15. When the bath depth is 700 mm, the mixing degree decreases profoundly to a range between 0.5 and 1.0, which is 50% lower compared with the case of Scheme A. Lower mixing degrees can also be found when the bath height is 500 mm. Because the upward flow caused by the bubble plume is coincident with the teeming flow from the inlet nozzle, the upward water flow is enhanced compared with the other two cases; this due to the interaction between the flow caused by the bubble plume and the flow due to teeming and, in turn, the resulting dissipation of energy that is otherwise used to stir the bath. The result of applying Scheme A shows that there is relatively poor overlapping between the gas and metal streams. This gives rise to more energy dissipation for bath stirring, especially between gas streams, and it explains why two plugs symmetrically placed in a ladle are not recommended. Consequently, applying Scheme C is favorable for the current ingot teeming process if bath stirring is a concern. Moreover, as the bubble plume is located at the center of the geometry of the ingot mold, bubbles could be efficiently prevented from being captured by the solidified shell.

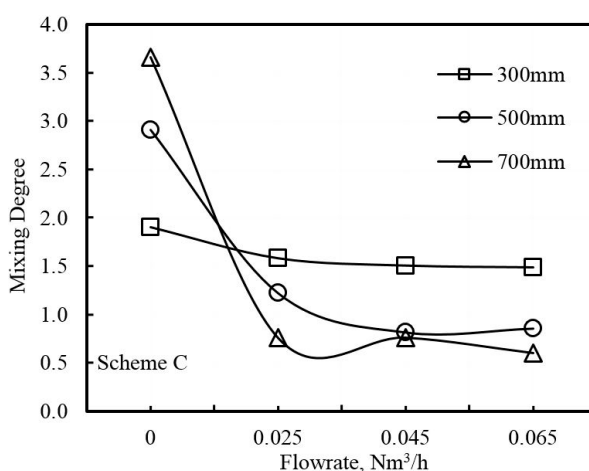


Figure 15. Mixing degree as a function of bottom blowing flowrate using Scheme C.

In addition, by comparing the analysis results shown in Figures 13–15, the mixing degrees, which range from 1.5 to 2.0 for gas flowrates increasing from 0 to 0.065 Nm³/h, suggest that the applied bottom blowing schemes do not show strong effects on the mixing behaviors when the bath depth is low (300 mm) because the rising distance of the bubbles from the bottom to the surface is relatively short. As a result, bubbles only have a short time to interact with the liquid in the bath, thus contributing less stirring energy.

4. Conclusions

The purpose of the current study was to design a method to explore the stirring of a dynamic bath and to determine a data analysis method to evaluate the data acquired from the experiment. With this method, the effects of different bottom blowing schemes on the bath stirring process were investigated. On the basis of the experimental results and discussion, the conclusions are summarized as follows.

The new analysis method for the bath mixing process is able to successfully reveal the relationship among blowing schemes, blowing flowrates, and bath depths.

The tracer flow patterns, together with the mixing degree analysis, suggest that there are different flow behaviors when the bath depth changes during the teeming process. The bath is weakly stirred without gas blowing when the depth is high.

The mixing degree results show that the applied bottom blowing schemes do not have strong effects on the mixing behaviors when the bath depth is small, while different bottom blowing schemes result in different bath stirring behaviors when the bath depth increases. For better bath stirring, application of the concentric circular annulus (Scheme C) is recommended for the ingot casting process. Compared with the bottom blowing schemes of A and B, a lower mixing time degree (0.5–1.5) can be obtained for an initial bath depth of 500 and 700 mm by applying the circular annulus blowing.

The new data analysis method used for the bath stirring process proves to be useful for expanding our understanding of how to best investigate a stirred bath with dynamic bulk liquid conditions; considering the history of the data during the measurement is beneficial, although a relative comparison can only be done for a specific system. It is also recommended that the new method be applied in a system where the bath mixing is plays an important role, and the bath volume changes during the process. In addition, since the bath depth is variable, the location at which to place the probe is a non-ignorable problem that needs attention to evaluate the effects of the probe location on the measurement results when the method is applied in other similar studies, even this factor does not affect the current study.

Author Contributions: Data curation, P.N.; Methodology, X.Z. and L.Z.; Resources, N.D.; Writing—original draft, X.Z.; Writing—review & editing, N.D.

Funding: The research work in this paper is supported by the National Natural Science Foundation of China (No.51704006 and No.51574069).

Conflicts of Interest: The authors declare no conflict of interest.

References

1. Zhang, M.J.; Gu, H.Z.; Huang, A.; Zhu, H.X.; Deng, C.J. Physical and mathematical modeling of inclusion removal with gas bottom-blowing in continuous casting tundish. *J. Min. Metall. Sect. B*. **2011**, *47*, 37–44. [[CrossRef](#)]
2. Wang, L.T.; Zhang, Q.Y.; Deng, C.H.; Li, Z.B. Mathematical model for removal of inclusion in molten steel by injecting gas at ladle shroud. *ISIJ Int.* **2005**, *45*, 1138–1144. [[CrossRef](#)]
3. Zhang, L.F.; Aoki, J.; Thomas, B.G. Inclusion removal by bubble floatation in a continuous casting mold. *Metall. Mater. Trans. B* **2006**, *37B*, 361–379. [[CrossRef](#)]
4. Eriksson, R.; Jonsson, L.; Jönsson, P.G. Effect of entrance nozzle design on the fluid flow in an ingot mold during filling. *ISIJ Int.* **2004**, *44*, 1358–1365. [[CrossRef](#)]
5. Hallgren, L.; Takagi, S.; Tilliander, A.; Yokoya, S.; Jönsson, P.G. Effect of nozzle type and swirl on flow pattern for initial filling conditions in the mould for uphill teeming. *Steel Res. Int.* **2007**, *78*, 254–259. [[CrossRef](#)]

6. Tan, Z.; Ersson, M.; Jönsson, P.G. Modeling of initial mold filling with utilization of swirl blades. *ISIJ Int.* **2012**, *52*, 1066–1071. [[CrossRef](#)]
7. Bai, H.; Ersson, M.; Jönsson, P.G. An Experimental and numerical study of swirling flow generated by turboswirl in an uphill teeming ingot casting process. *ISIJ Int.* **2016**, *56*, 1404–1412. [[CrossRef](#)]
8. Singh, V.; Kumar, J.; Bhanu, C.; Ajmani, S.K.; Dash, S.K. Optimisation of the bottom tuyeres. *ISIJ Int.* **2007**, *47*, 1605–1612. [[CrossRef](#)]
9. Murthy, G.G.K.; Mehrotra, S.P.; Ghosh, A. Experimental investigation of mixing phenomena in a gas stirred liquid bath. *Metall. Mater. Trans. B* **1988**, *19*, 839–850. [[CrossRef](#)]
10. Komarov, S.V.; Itoh, K.; Sano, M.; Blinov, K.A. Mixing phenomena in a ladle bath stirred by gas jets through side and inclined nozzles. *ISIJ Int.* **1993**, *33*, 740–747. [[CrossRef](#)]
11. Yeoh, S.L.; Papadakis, G.; Yianneskis, M. Determination of mixing time and degree of homogeneity in stirred vessels with large eddy simulation. *Chem. Eng. Sci.* **2005**, *60*, 2293–2302. [[CrossRef](#)]
12. Vichare, N.P.; Gogate, P.R.; Dindore, V.Y.; Pandit, A.B. Mixing time analysis of a sonochemical reactor. *Ultrason. Sonochem.* **2001**, *8*, 23–33. [[CrossRef](#)]
13. Ascanio, G. Mixing time in stirred vessels: A review of experimental techniques. *Chin. J. Chem. Eng.* **2015**, *23*, 1065–1076. [[CrossRef](#)]
14. Kouda, T.; Yano, H.; Yoshinaga, F.; Kaminoyama, M.; Kamiwan, A.M. Characterization of non-newtonian behavior during mixing of bacterial cellulose in a bioreactor. *J. Ferment. Bioeng.* **1996**, *82*, 382–386. [[CrossRef](#)]
15. Arratia, P.E.; Muzzio, F.J. Planar laser-induced fluorescence method for analysis of mixing in laminar flows. *Ind. Eng. Chem. Res.* **2004**, *43*, 6557–6568. [[CrossRef](#)]
16. Holmes, D.B.; Voncken, R.M.; Dekker, J.A. Fluid flow in turbine-stirred, baffled tanks—I: Circulation time. *Chem. Eng. Sci.* **1964**, *19*, 201–208. [[CrossRef](#)]
17. Poulsen, B.R.; Iversen, J.J.L. Mixing determinations in reactor vessels using linear buffers. *Chem. Eng. Sci.* **1997**, *52*, 979–984. [[CrossRef](#)]
18. Zhou, X.; Ersson, M.; Zhong, L.; Jönsson, P.G. Optimization of combined blown converter process. *ISIJ Int.* **2014**, *54*, 2255–2262. [[CrossRef](#)]
19. Zhou, X.; Ersson, M.; Zhong, L.; Yu, J.; Jönsson, P.G. Mathematical and physical simulation of a top blown converter. *Steel Res. Int.* **2014**, *85*, 273–281. [[CrossRef](#)]
20. Zhang, Q.; Yong, Y.; Mao, Z.-S.; Yang, C.; Zhao, C. Experimental determination and numerical simulation of mixing time in a gas—Liquid stirred tank. *Chem. Eng. Sci.* **2009**, *64*, 2926–2933. [[CrossRef](#)]
21. Zhong, L.; Zhou, X.; Jiang, P.; Wang, H.; Pang, L.; Hao, P. Physical and mathematical simulations for molten steel flow in a large ingot casting process with double bottom argon bubbling porous beams. *Ironmak. Steelmak.* **2017**. [[CrossRef](#)]

